

# LIBRA: Enabling Workload-aware Multi-dimensional Network Topology Optimization for Distributed Training of Large AI Models

William Won\*, Saeed Rashidi\*<sup>§</sup>, Sudarshan Srinivasan<sup>†</sup>, and Tushar Krishna\*

\*Georgia Institute of Technology, Atlanta, GA, USA

<sup>†</sup>Intel, Bangalore, Karnataka, India

\*william.won@gatech.edu \*saeed.rashidi@gatech.edu <sup>†</sup>sudarshan.srinivasan@intel.com \*tushar@ece.gatech.edu

**Abstract**—As model sizes in machine learning continue to scale, distributed training is necessary to accommodate model weights within each device and to reduce training time. However, this comes with the expense of increased communication overhead due to the exchange of gradients and activations, which become the critical bottleneck of the end-to-end training process. In this work, we motivate the design of multi-dimensional networks within machine learning systems as a cost-efficient mechanism to enhance overall network bandwidth. We also identify that optimal bandwidth allocation is pivotal for multi-dimensional networks to ensure efficient resource utilization. We introduce LIBRA, a framework specifically focused on optimizing multi-dimensional fabric architectures. Through case studies, we demonstrate the value of LIBRA, both in architecting optimized fabrics under diverse constraints and in enabling co-optimization opportunities.

**Index Terms**—multi-dimensional networks, distributed training, large language models, quadratic programming

## I. INTRODUCTION

The demand for sophisticated, large-scale Machine Learning (ML) models is greater than ever. This is exemplified by recent Large Language Models (LLMs) powering tools like OpenAI ChatGPT [1], Google Gemini [2], and Microsoft Copilot [3]. The proliferation of ML-based applications has led to a growing trend of designing specialized high-performance Computing (HPC) systems to train ML models. Examples include Google Cloud TPU [4], Intel Habana HLS [5], Meta Research SuperCluster [6], Tesla Dojo [7], Cerebras CS-2 [8], and Tensorrent Galaxy [9]. Such Artificial Intelligence (AI) systems possess two notable features: (i) Neural Processing Units (NPU, e.g., GPUs or custom ASICs [9]–[12]) designed to efficiently execute compute operations, and (ii) specialized network fabrics to scale-up and scale-out the system to thousands of NPUs. It is important to note that many of these AI systems are optimized at design-time for specific models of interest. For instance, the Meta ZionEX cluster [13] is specifically designed for accelerating large-scale DLRM [14] training. While substantial research has been conducted on the architecture of NPUs [15], [16], *there has been limited work on architectural decisions for the custom fabric*, which constitutes the central focus of this work.

AI models, especially LLMs, consist of billions to trillions of parameters (i.e., weights) that need to be distributed across

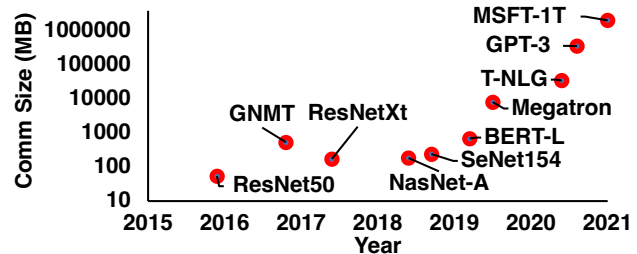


Fig. 1. Communication sizes (FP16 as the datatype) for ML model training across 1,024 NPUs. The parallelization strategy of Turing-NLG and smaller workloads are data parallel (minibatch size of 32), while GPT-3 and MSFT-1T use both tensor and data parallelism.

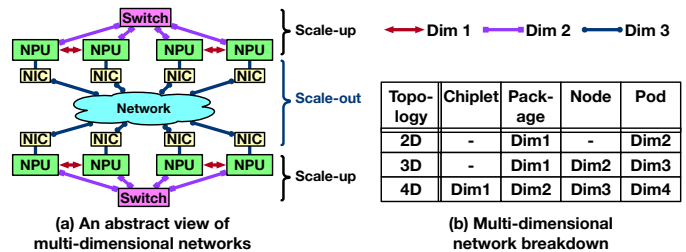


Fig. 2. (a) An abstract view of multi-dimensional networks. (b) An example of physical connotation assigned to 2–4D networks.

NPUs since they cannot fit within the memory of a single device.<sup>1</sup> The synchronization of model activations and gradients during training leads to heavy communication among NPUs. As shown in Fig. 1, the total communication size for large model training can span GBs to TBs. Consequently, communication becomes one of the major bottlenecks in distributed training [19]–[23]. This naturally necessitates driving higher network bandwidth (BW) resources per NPU to efficiently process the massive volume of communication during training.

Therefore, AI clusters in data centers today most commonly leverage two-dimensional (i.e., 2D) network fabrics to achieve high network BW. In the first dimension (i.e., Dim), they employ custom rack-to-rack links (e.g., XeLink [24] or NVLink [25]) to scale-up a node, enabling peer-to-peer communication among NPUs. The second dimension is the conventional scale-out fabric, which employs Network Inter-

<sup>1</sup>Even if a model fits within a single NPU, the raw compute requirement to train a model necessitates distributed training. For example, GPT-3 [17] takes 355 years to be trained using a single NVIDIA V100 GPU [18].

<sup>§</sup>Current affiliation: Hewlett Packard Enterprise [saeed.rashidi@hpe.com]

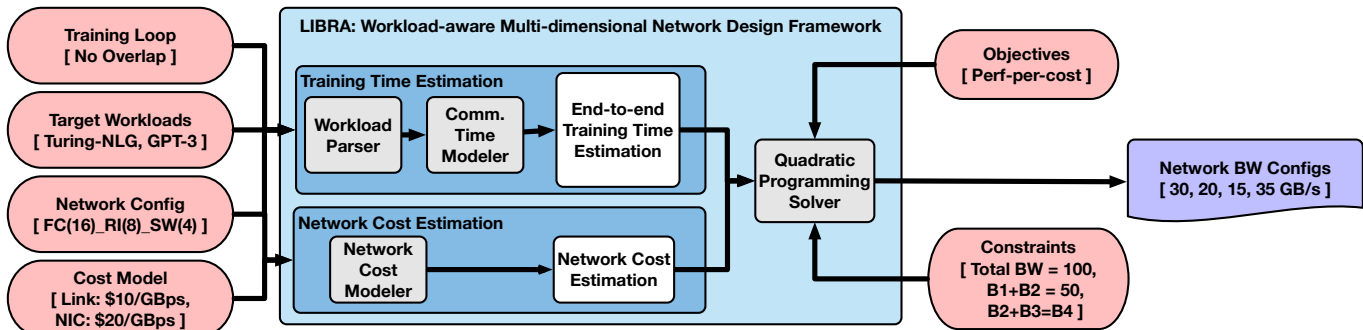


Fig. 3. The architecture of LIBRA, a workload-aware multi-dimensional network BW optimization framework. Inputs to the LIBRA framework are represented in ovoids, with corresponding example values shown in square brackets. LIBRA estimates the end-to-end training time based on the provided network shape, training loop, and target workloads. Additionally, it calculates the cost of a network using a specified cost model and network shape. Subsequently, LIBRA searches for the optimal network BW configuration that maximizes the given objective while adhering to designated design constraints.

face Cards (NICs) using technologies such as Ethernet [26] or InfiniBand [27]. However, as AI models continue to scale at an unprecedented rate [28], next-generation AI systems demand even higher network BW, and addressing this challenge remains an open problem. A naive approach would be to increase the individual BW of the two dimensions. However, it is pivotal to note that physical and management constraints, such as limited pin counts allotted per each network dimension, electrical SerDes constraints, signaling, and power consumption, cap the potential network BW achievable per each network dimension [29]. For example, while we can expect some further increase in BW across generations of scale-up and scale-out links, NVLink technology today only reaches a maximum of 450 GB/s [25]. This is true even with transitioning to alternative technologies that may offer higher BW, such as advanced wafer-scale packaging [30]–[32] or photonics [33], [34], since additional physical constraints like thermals and reliability still apply as well as expensive manufacturing costs (at least today). In summary, there is no single technology that can provide high network BW within a single network dimension. This is evident from the diverse fabrics used in AI systems today: Intel leverages XeLink and InfiniBand technologies [35], NVIDIA uses NVLink, NVSwitch, and InfiniBand NICs [36]–[38], and Cerebras [8] and Tesla [7] utilize Wafer-scale and Chipllets.

We believe that a promising approach to enhance the BW per NPU is to (i) explicitly add more network dimensions, and (ii) leverage a mixture of fabric technologies. An abstract view of such multi-dimensional fabrics for AI systems is demonstrated in Fig. 2. By having multiple network dimensions, we can overcome the constraint of limited BW of each network dimension and drive overall higher network BW per NPU. For example, Google Cloud TPUv4 [33] employs a 3D point-to-point electrical network augmented by a photonic network dimension in order to drive more network resources [33]. Even when employing a multi-dimensional network to allocate equal BW resources per NPU, it can still achieve a higher performance-per-cost (i.e., perf-per-cost) design point. This is attributable to the load-reducing nature of the multi-rail communication algorithm, which enables substituting expensive network resources with more cost-efficient technologies.

This multi-dimensional network scheme opens up a new fabric architecture optimization problem that this work aims to solve: *how to determine BW distribution across different dimensions at design-time, under diverse technology-driven dollar cost and BW constraints, while enabling high performance across multiple AI workloads?* As we show in this work, judicious optimization of network BW at design-time is necessary to enable co-optimization and scheduling opportunities at runtime. Otherwise, BW resources augmented by leveraging multi-dimensional topologies may be underutilized, resulting in inefficiencies in communication and training slow-down [39]. Resource allocation design is always a challenging problem, akin to other design challenges like sizing scratchpads or caches. However, unlike general-purpose HPC applications, communication patterns (e.g., communication types, sizes, and the group of NPUs involved) for ML applications can be predetermined when the parallelization strategy of a workload is set. Therefore, focusing on AI workloads enables us to adopt a more systematic workload-aware approach.

To this end, we propose **LIBRA: Leveraging Intelligent Bandwidth Resource Allocation for multi-dimensional networks**.<sup>2</sup> LIBRA is a workload-aware, multi-dimensional network optimization framework at design-time.<sup>3</sup> The architecture of LIBRA is summarized in Fig. 3. Given a set of target Deep Neural Network (DNN) models, fabric technology options, and design constraints, LIBRA can swiftly estimate the training performance and propose the optimal network BW design point that maximizes performance or perf-per-cost. Through case studies, we demonstrate that LIBRA can be used for two primary purposes: (i) optimizing the multi-dimensional network architecture for a family of target workloads, and (ii) exploring co-optimization opportunities, such as designing networks alongside target workload parallelizations or runtime-based training scheduling techniques. To the best of our knowledge, LIBRA is the first workload-aware constrained-optimization framework for AI systems fabric design.

<sup>2</sup>Libra also symbolizes *balance* in Latin, aligning with this work of judiciously allocating and harmonizing BW resources across dimensions.

<sup>3</sup>LIBRA yields an optimized network *design* targeted for a specific set of workloads. We use the term *design-time* to contrast LIBRA, as a toolchain, with runtime-based methodologies (e.g., schedulers or load balancers).

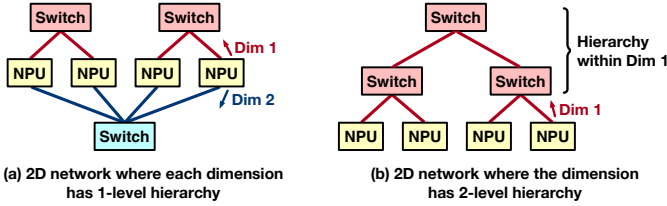


Fig. 4. (a) An example of a switch-based 2D network. (b) Example 1D topology, which utilizes a 2-level hierarchical switch in Dim 1.

## II. BACKGROUND

### A. Multi-dimensional Network

A *multi-dimensional network* is defined as a network topology where each NPU has multiple independent connectivity options, which can be accessed in parallel to communicate with other NPUs. An abstract view of the multi-dimensional network is illustrated in Fig. 2(a). This concept is equivalent to the definition of multi-rail networks [40], [41]. In Fig. 2(b), physical technology connotations are assigned to each network dimension as an illustrative example for 2–4D networks.<sup>4</sup> We introduce Chiplet, Package, Node, and Pod, inspired by emerging technology and system trends. Chiplet represents an NPU chip. Package consists of one or more Chiplets interconnected via Multi-chip Module (MCM) packaging [31], [42]. A Pod is an inter-server scale-out unit used in some platforms today, typically interconnected through NICs [5]. A Node constructs a server unit by connecting multiple Packages through an inter-board network.

It’s worth noting that in our terminology, a network *dimension* is distinct from adding a *hierarchy* within a network dimension. Each dimension of the network is directly accessible to the NPU (via explicit ports/pins) in parallel. In contrast, within a dimension, the implementation may choose to use a hierarchy, such as a hierarchy of switches instead of a single large switch. This distinction is depicted in Fig. 4. While both topologies utilize three physical switches, Fig. 4(a) represents a 2D network since NPUs have two distinct switch-based networks accessible in parallel, whereas Fig. 4(b) showcases a 1D topology using a 2-level switch hierarchy within Dim 1.

### B. Distributed Training

**Parallelization Strategy.** Modern foundation models, along with other large models, often have a substantial memory footprint during training, which exceeds the capacity of a single NPU memory [43]. To address this issue, the model and training dataset need to be sharded and distributed across multiple NPUs. The *parallelization strategy* governs how the model and dataset are divided and placed. There are two main parallelization strategies: Tensor Parallelism (TP) and Data Parallelism (DP). TP divides the model and distributes them across NPUs, reducing the memory requirement of each NPU during training [44]. We use TP- $n$  to denote that the model is sharded in  $n$ -way. DP distributes the training dataset to boost the training throughput [44]. We use DP- $n$  to indicate

<sup>4</sup>This example physical connotation is used for evaluation purposes in this paper. Still, LIBRA remains flexible and supports arbitrary dimensionalities.

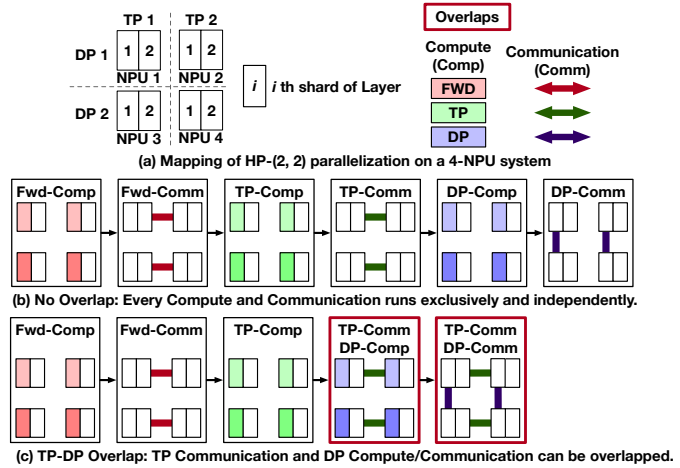


Fig. 5. Examples of training loops. (a) HP-(2,2) parallelization strategy (b) A training loop without any overlap (No Overlap) (c) A training loop with TP and DP running concurrently (TP-DP Overlap).

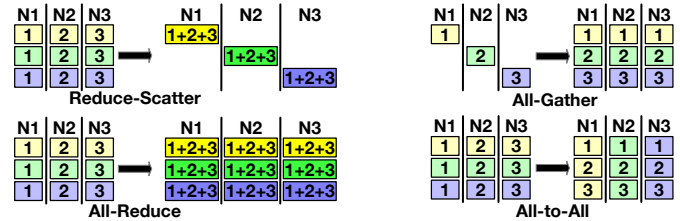


Fig. 6. Common collective patterns (N denotes an NPU).

that the training dataset is split into  $n$  separate groups. TP and DP are orthogonal and can be combined, resulting in a hybrid parallelism (HP) scheme. We use HP-( $m, n$ ) to denote the mixture of TP- $m$  and DP- $n$ . In the HP-( $m, n$ ) setup, the training dataset is first split into  $n$  sets, and each set is fed into the group where the model is  $m$ -way sharded. Consequently, HP-( $m, n$ ) requires a total of  $m \times n$  NPUs. We leverage sophisticated hybrid parallelization schemes such as Megatron-LM [45], combined with the ZeRO-2 optimizer [43].

**Training Loop.** Each parallelization strategy necessitates devices to communicate and synchronize dispersed information. For instance, TP requires input activations and input gradients to be communicated, while DP necessitates the synchronization of weight gradients. The *training loop* defines the ordering and scheduling of computation and communication during the training process. As shown in Fig. 5, we provide two examples of training loops for HP-(2,2) of a single-layer model. In Fig. 5(b), there are no overlaps between the computation and communication stages. In contrast, Fig. 5(c) allows the overlap of TP communication and DP computation and communication, resulting in a shorter training time.

### C. Collective Communication

**Topology-aware Collective Algorithms.** Communications required by parallelization strategies are managed through collective communications (i.e., collectives). Common collectives in distributed training are illustrated in Fig. 6. The most prominent collective in distributed training is All-Reduce [19]. It is logically equivalent to Reduce-Scatter followed by an

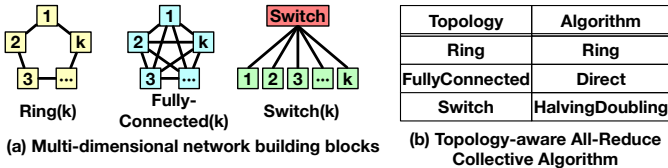


Fig. 7. (a) Multi-dimensional network building blocks. (b) their corresponding topology-aware All-Reduce algorithm.

All-Gather [46]. In certain cases of TP, like embedding tables [14], All-to-All is required. Real systems execute collectives using collective communication algorithms through Collective Communication Libraries (CCLs) [47], [48]. For example, Ring, Direct, and Recursive Halving-Doubling are commonly used All-Reduce algorithms [49]. These algorithms are *topology-aware collective algorithms* designed for Ring, FullyConnected, and Switch networks, respectively, ensuring that they do not introduce link contention when running on their respective physical topologies. Fig. 7 lists common network building blocks and their corresponding topology-aware collective algorithms.

**Multi-rail Collective Algorithm.** Basic collective algorithms are not ideally suited for direct use over multi-dimensional networks. For instance, the Direct collective algorithm performs well on a FullyConnected network, but the physical connectivity of multi-dimensional networks often does not meet such expectations. Consequently, heavy network contention and oversubscription over low-BW links can occur, leading to significant underutilization of network BW. To address this issue, *multi-rail* collective algorithms have been proposed to fully leverage the resources of multi-dimensional networks [46], [50], which is the approach adopted in LIBRA. A multi-rail collective algorithm capitalizes on the inherent nature of multi-dimensional networks, where basic network building blocks are stacked up. Therefore, it executes basic collective algorithms in sequence. For example, to perform an All-Reduce collective on an  $N$ -dimensional network:

- Run Reduce-Scatter on Dim 1. Then, run Reduce-Scatter on Dim 2. These Reduce-Scatter jobs, in ascending order, continue up to Dim  $N$  ( $N$  Reduce-Scatter stages).
- Perform All-Gather on Dim  $N$ , then execute All-Gather on Dim  $N - 1$ . This All-Gather stage continues, in descending order, down to Dim 1 ( $N$  All-Gather stages).

In summary, the multi-rail All-Reduce collective algorithm involves a total of  $2N$  stages. Within each stage, each dimension utilizes its corresponding topology-aware collective algorithm. This approach guarantees that the overall collective operation runs in a contention-free manner. An example All-Reduce on a  $3 \times 2$  (2D) network is illustrated in Fig. 8.

### III. MOTIVATION AND CHALLENGES

#### A. Technology Constraints of a Network Dimension

ML Training platforms commonly utilize 2D networks that leverage two technologies: (i) a high-BW proprietary network to connect multiple NPUs within a server node (i.e., *scale-up*) and (ii) NICs to connect NPUs across server nodes (i.e., *scale-out*) [13], [36], [51], [52]. However, increasing

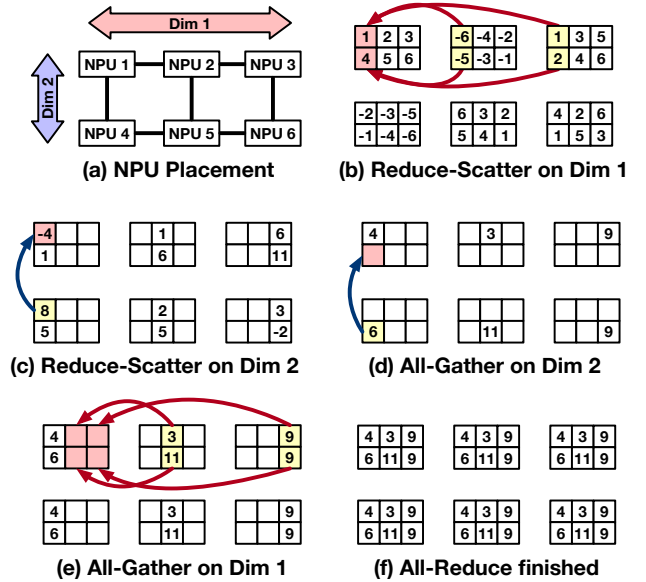


Fig. 8. All-Reduce example on a  $3 \times 2$  (2D) network. (a) NPU placement (b–c) Reduce-Scatter phase (d–e) All-Gather phase (f) All-Reduce collective finished. Arrows represent the traffic of chunks received by NPU 1 for each stage.

the raw network BW of each dimension in such setups is often challenging and expensive. This limitation arises due to the fundamental physical constraints imposed by the link technologies and their associated costs, such as pin counts, manufacturing, thermals, power, and area considerations [29]. For instance, the current NVLink technology [25] can provide up to 450 GB/s per NPU, and the state-of-the-art NIC can drive up to 50 GB/s [26].

#### B. Opportunity: Multi-dimensional Networks

In large model distributed training, a multi-dimensional topology composed of multiple network technologies can be an effective solution. There are two key benefits that such topologies provide in the context of DNN training.

**Higher Aggregated BW.** Simultaneously leveraging multiple network technologies, including chiplets [31] and photonics [33], [34], offer an opportunity to further increase aggregate BW per NPU by introducing additional network dimensions between NPUs either on a package [31] or on a board [33].

**Higher Perf-per-cost.** As chunks are successively *reduced* throughout the stages of the multi-rail Reduce-Scatter phase, the volume of communication progressively decreases at each network dimension. This reduction in communication size is depicted in Fig. 8. NPU 1 first receives 4 chunks from its neighbors through Dim 1. However, since these messages are reduced into a single chunk, the second Reduce-Scatter stage through Dim 2 only requires receiving 1 chunk. As a result, having more network dimensions significantly reduces the message size once it reaches higher network dimensions. This enables organizing a multi-dimensional network in a way that cheaper network technologies (i.e., scale-up) drive higher network BW resources in lower network dimensions. Expensive network technologies (e.g., NICs or photonics) can establish higher network dimensions while providing limited

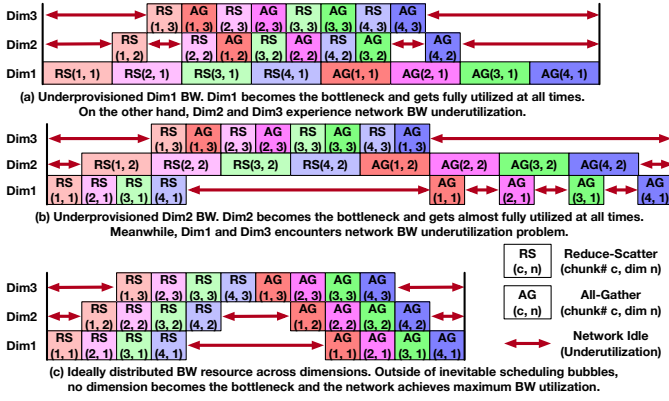


Fig. 9. Running All-Reduce with 4 chunks on 3D networks with different BW allocations.

BW resources, benefiting from the reduced communication burden enabled by multi-dimensionality. Even when allocating equal BW resources per NPU, this architectural design yields significant perf-per-cost improvements by substituting expensive technologies with more cost-effective resources.

### C. Challenge: Design-time Consideration of Network BW

Realizing a multi-dimensional architecture is a challenging task since the allocation of physical BW across network dimensions at design time can significantly impact the runtime performance. Consequently, appropriately sizing the BW of each network dimension becomes crucial to avoid overprovisioning or underprovisioning network resources. This can be exemplified by the scenario in Fig. 8. The payload size of Dim 2 is only a quarter of Dim 1’s due to the reduction phase in Dim 1. Consequently, the *BW requirement* of Dim 2 is only 1/4 of Dim 1’s. If the *physical network BW* of Dim 2 is larger than 1/4 of Dim 1’s, then Dim 2’s BW resource is overprovisioned, leading to underutilization. Conversely, if Dim 2’s BW is less than 1/4 of Dim 1’s, Dim 2 becomes the bottleneck and Dim 1’s network resource will be underexploited. A collective communication usually consists of multiple chunks that run in a pipelined manner [53]. Fig. 9 provides a generalized scenario by using a 3D network. In Fig. 9(a), Dim 1’s physical BW is smaller than its requirement, making Dim 1 the communication bottleneck and leading to significant underutilization of other dimensions (Dim 2 and Dim 3). Similarly, Fig. 9(b) depicts a case where Dim 2’s BW is underprovisioned, resulting in extensive network underutilization of Dim 1 and Dim 3. If we can judiciously design a multi-dimensional network with such consideration, the network utilization can be maximized, as shown in Fig. 9(c). The potential benefits of using workload-aware multi-dimensional networks are demonstrated in Fig. 10. The plot shows the normalized runtime to train the MSFT-1T model, where each NPU has a 300 GB/s aggregated BW per NPU, but assuming different network BW utilization ratios. In the baseline EqualBW configuration (all network dimensions have an equal amount of BW, explained in Sec. V-B), the network BW utilization was only 57.53%, 39.02%, and 66.74% for 2D, 3D, and 4D networks, respectively. By using a workload-aware

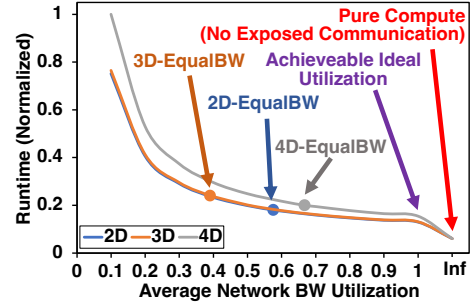


Fig. 10. The normalized end-to-end training time of MSFT-1T on 2D, 3D, and 4D topologies with 300 GB/s per NPU. Average network BW utilization was 53.11% (66.74% max). We can achieve 1.83× maximum speedup if we can reach 100% BW utilization.

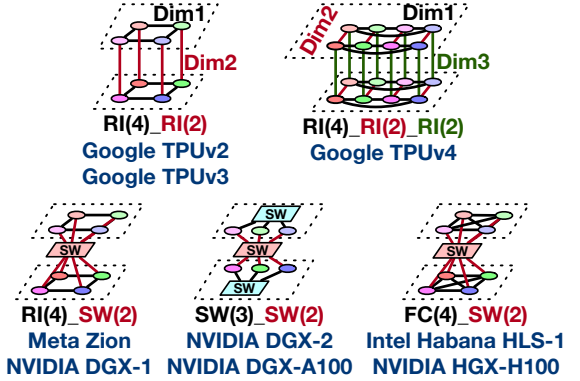


Fig. 11. Examples of 2–3D networks and their corresponding names in the notation used in this work are provided. To demonstrate the expressiveness of the representation in capturing real systems, corresponding ML HPC clusters that utilize equivalent network shapes are also listed.

network BW configuration optimized for the target MSFT-1T model, we can maximize the network BW utilization and theoretically achieve training speedups of 1.39×, 1.83×, and 1.29×, respectively. This result emphasizes the critical role of network BW distribution across dimensions for AI collectives.

## IV. LIBRA

In this section, we introduce LIBRA: a workload-aware, design-time multi-dimensional network optimization framework. We explain how LIBRA can model collective communications, large model distributed training, and optimize the network BW of multi-dimensional topologies. LIBRA repository is open-sourced and can be publicly accessed.<sup>5</sup>

### A. Multi-dimensional Network Representation

In this work, we utilize the multi-dimensional network representation from [54]. We adopt three unit topologies as building blocks for each network dimension: Ring (RI), Fully-Connected (FC), and Switch (SW), as shown in Fig. 7. Multi-dimensional networks can be represented by stacking the building blocks together alongside the corresponding network size. For example, RI(4)\_RI(4)\_RI(4) represents a 3D Torus network with 64 NPUs. To demonstrate the capability to capture HPC networks in deployment, Fig. 11 depicts five

<sup>5</sup><https://github.com/astra-sim/libra>

examples of 2–3D networks captured in this taxonomy and their corresponding ML HPC clusters in use. Although not shown, the notation is flexible and can be leveraged to capture multi-dimensional networks with four dimensions or more.

### B. Problem Statement and Constraints

LIBRA is a design-time framework to construct an HPC network optimized for AI training. Given a set of target workloads and a multi-dimensional network representation, LIBRA performs optimization to yield the best network BW configuration. The optimization process aims to maximize specific objectives such as training performance or perf-per-cost. LIBRA, throughout optimization, ensures that the network BW configuration adheres to the user-defined design constraints, such as fixed BW per NPU, BW limit for a specific dimension, or limited total network cost.

### C. Modeling Distributed Training

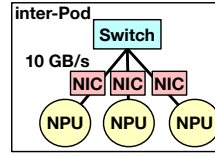
In order to optimize for the best BW configuration of a multi-dimensional network, LIBRA estimates the end-to-end training time as a function of network BW. To achieve this, LIBRA first models collective communications as a function of network BW. Consider a scenario where we run an  $m$ -sized All-Reduce operation on a 2D ( $n_1 \times n_2$ ) network with  $B_1$  and  $B_2$  for its two dimensions' BW. Mathematically, the nature of multi-rail All-Reduce results in the traffic volume of  $\frac{2m(n_1-1)}{n_1}$  and  $\frac{2m(n_2-1)}{n_1 n_2}$  transferred by each dimension, respectively. Taking into account the BW of each dimension, and considering the bottlenecking dimension determines the collective time (as shown in Fig. 9), the All-Reduce time is  $\max\left(\frac{2m(n_1-1)}{n_1 B_1}, \frac{2m(n_2-1)}{n_1 n_2 B_2}\right)$ . Similarly, Reduce-Scatter and All-Gather can be modeled as  $\max\left(\frac{m(n_1-1)}{n_1 B_1}, \frac{m(n_2-1)}{n_1 n_2 B_2}\right)$  since the communication volume halves compared to All-Reduce. Finally, All-to-All time is computed as  $\max\left(\frac{m(n_1-1)}{n_1 B_1}, \frac{m(n_2-1)}{n_2 B_2}\right)$  due to the absence of chunk reduction. Such models can be further generalized as the network dimensionality increases. Ultimately, LIBRA estimates all communication times as functions where the sole parameter is the network BW configuration.

The end-to-end model training can be captured by leveraging such communication representation. The training loop depicted in Fig. 5(b) has no overlap among the computation and communication stages. Therefore, the end-to-end execution time is estimated by simply aggregating all compute and communication delays. Specifically, the forward pass takes  $\sum_{l \in \text{layer}} (\text{Fwd\_Compute}_l + \text{Fwd\_Comm}_l)$  time. Note that  $\text{Fwd\_Compute}_l$  is BW-independent and  $\text{Fwd\_Comm}_l$  is a function of network BW. Similarly, the backward pass takes  $\sum_{l \in \text{layer}} (\text{TP\_Compute}_l + \text{TP\_Comm}_l + \text{DP\_Compute}_l + \text{DP\_Comm}_l)$ . If there are overlaps in complex training loops, they can easily be reflected in the end-to-end time estimation. For example, training loop Fig. 5(c) assumes that  $\text{TP\_Compute}$  is fully exposed but overlapping  $\text{TP\_Comm}$  with  $\text{DP\_Compute}$  and  $\text{DP\_Comm}$  is possible. Then, each layer's backward pass will take  $\text{TP\_Compute} + \max(\text{TP\_Comm}, \text{DP\_Compute} + \text{DP\_Comm})$  time. The end result is LIBRA estimating and

TABLE I

COST MODEL FOR NETWORK COST EVALUATION. DOLLAR-COST OF EACH NETWORK COMPONENT PER GB/S IS SHOWN. THE VALUES ARE DERIVED FROM MOST CURRENT AVAILABLE DATA [5], [11], [26], [52], [57], [58]. WE USED THE LOWEST VALUE OF EACH ENTRY FOR EVALUATION.

(\$/GBps)	Link	Switch	NIC
Inter-Chiplet	2.0	-	-
Inter-Package	4.0 – 5.2	13.0	-
Inter-Node	4.0 – 5.2	13.0	-
Inter-Pod	7.8 – 16	18.0 – 69.6	31.6 – 144



- Link:  $\$7.8 \times 10 \text{ GB/s} \times 3 = \$234$
- Switch:  $\$18.0 \times 3 \text{ (radix)} \times 10 \text{ GB/s} = \$540$
- NIC:  $\$31.6 \times 10 \text{ GB/s} \times 3 = \$948$
- Total Network Cost =  $\$234 + \$540 + \$948 = \$1,722$

Fig. 12. Example cost modeling of a 3 NPU switch network. The network Cost Model used for the cost modeling is shown in Table I.

capturing the training performance of a DNN model as a function of network BW, which can then be optimized.

**LIBRA Modeling:** In the current LIBRA modeling, we disregarded the impact of link latencies or NPU performance implications (e.g., memory access BW or reduction performance). Large-model training commonly involves large traffic volumes, making communication highly network BW-bound [55]. This allows modeling communication performance in network BW configuration to be a feasible option. In general, accurately modeling collective communications with more intricate equations has been the focus of recent endeavors, which is orthogonal to this work since LIBRA can incorporate such modeling and still optimize for network BW configurations.

**In-network Collective:** The offloading of collectives to the network switches has been a subject of research [20] and commercial developments [38], [56]. In essence, in-network collective offloading effectively reduces the communication time of Dim  $i$  to  $\frac{m}{n_1 n_2 \dots n_{i-1} B_i}$ .

**Parallelization Strategy:** Intricate parallelization strategies, including Pipeline Parallelism, periodically involve non-collective communication patterns such as direct NPU-to-NPU message transfers. Such operations could still be captured in terms of network BW (e.g.,  $\frac{m}{B_i}$ ) and can be leveraged in estimating end-to-end performance.

### D. Modeling Network Cost

In addition to performance modeling, LIBRA can estimate the dollar cost of multi-dimensional networks. This estimation process relies on the network cost model, which is provided as an input parameter to LIBRA by the user. The reason for this is that network costs can vary significantly based on the technology and specific vendors and may also change over time.<sup>6</sup> To facilitate the analysis, we offer a default cost model (shown in Table I), derived from costs available in public citations. This default model is used for design-space exploration in this work. In this default cost model, Pod is defined as the unit for scale-out, meaning other network dimensions do not utilize NICs. For inter-Chiplet networks,

<sup>6</sup>For instance, the inter-node link costs can vary significantly across high-speed electrical [24], [25] vs. photonic [33].

we assume Chiplelets are always connected peer-to-peer, thereby eliminating the need for switches. Fig. 12 depicts an example cost analysis based on this default cost model.

### E. Optimizing Multi-dimensional Network

With the provided modeling capabilities, LIBRA can optimize the network BW for a target DNN training task, leading to the ideal network BW allocation that achieves specific objectives, such as maximizing training performance. LIBRA utilizes a Quadratic Programming (QP) solver [59] to carry out the network optimization. Furthermore, LIBRA has the capability to optimize for a network that targets *multiple target workloads*, accommodating real-world training scenarios.

### F. Optimization Scheme

LIBRA supports two optimization objectives to yield different network BW design points, as discussed below.

**(i) PerfOptBW.** The PerfOptBW optimization scheme aims to maximize the model training performance. LIBRA’s QP solver disregards the network cost factor and the solver’s optimization objective is set to minimize the end-to-end training time.

**(ii) PerfPerCostOptBW.** PerfPerCostOptBW takes into account both network cost and performance. It multiplies end-to-end training time by the estimated network cost, to measure the (reciprocal of) perf-per-cost metric, for which the QP solver inside LIBRA is then configured to minimize.

In practice, we envision that AI training clusters will be *designed to handle a family of target workloads*, not just a single target. LIBRA is capable of designing a network aware of multiple target workloads. It is achieved by optimizing a *weighted sum of the end-to-end training time* of individual target workloads, where the weight represents the importance of the corresponding workload. This results in a network design point that is optimized towards multiple workloads. By accommodating multiple targets and considering their relative importance, LIBRA becomes a versatile tool for designing networks that can effectively handle various training scenarios.

LIBRA harnesses the power of a QP solver to find an ideal network design point, providing the flexibility to represent linear and quadratic constraints as desired by the system designer. For instance, if there is a restriction on the total network BW per NPU, it can be easily represented as  $\sum_i B_i \leq B$ , where  $B_i$  denotes the BW of Dim  $i$ . Similarly, to limit the inter-Pod dimension BW to 50 GB/s, this constraint is captured as  $B_4 \leq 50\text{GB/s}$ . The representation of constraints is highly adaptable, allowing for the addition of various flexible constraints of interest, such as  $B_1 + B_2 = 500\text{ GB/s}$  or  $B_1 \geq B_2 \geq B_3$ ,  $25 \leq B_3 \leq 150\text{ GB/s}$ . Multiple constraints can be applied simultaneously, enabling a comprehensive and customized network optimization.

## V. METHODOLOGY

### A. Simulation Infrastructure

LIBRA is a standalone framework aimed at aiding the design process for determining multi-dimensional network BW configurations. However, to profile and measure the performance

TABLE II  
WORKLOADS SPECIFICATIONS USED FOR ANALYSIS.

Workload	Params	TP Size
Turing-NLG	17B	1
GPT-3	175B	16
MSFT-1T	1T	128
DLRM	57M (MLP layers only)	Across all NPUs
ResNet-50	25.6M	1

TABLE III  
MULTI-DIMENSIONAL TOPOLOGIES USED FOR ANALYSIS.

Name	Shape
4D-4K	RI(4)_FC(8)_RI(4)_SW(32)
3D-4K	RI(16)_FC(8)_SW(32)
3D-512	SW(16)_SW(8)_SW(4)
3D-1K	FC(8)_RI(16)_SW(8)
4D-2K	RI(4)_SW(4)_SW(8)_SW(16)
3D-Torus	RI(4)_RI(4)_RI(4)

of networks designed by LIBRA, a simulation infrastructure is necessary to meticulously identify the practical implications. In this paper, we utilized ASTRA-sim distributed ML simulator [46], [54] for the identification of the LIBRA-generated networks’ training performance. ASTRA-sim enables executing complex DNN workloads, modeling complex network architecture, running various collective algorithms with chunk-level scheduling, and capturing compute-communication overlaps. **Validation.** ASTRA-sim is validated over multiple real ML systems and showed an error rate of 2.8–11.4% [60].

### B. Experimental Setup

**Baseline.** In this work, we use EqualBW as a straw-person baseline. The EqualBW scheme distributes the given BW resource  $B$  equally across all  $N$  dimensions, resulting in  $\frac{B}{N}$  allocated to each dimension. EqualBW is chosen as the baseline since it is a workload-agnostic allocation without performance considerations and an actual optimization process.

**Workloads.** We selected three transformer-based LLMs and two non-LLMs (recommendation and vision) [14], [61], [62] for evaluations in this paper. To distribute these models, we assumed ZeRO phase-2 optimizers [43]. The specifications of the selected models are provided in Table II. All communications are split into 64 chunks per collective.

**Compute Model.** The average efficacy of the A100 GPU [37] was measured to be 75% (i.e., 234 TFLOPS) and was used to estimate NPU compute times in the evaluation.

**Network Topologies.** We adopted different target multi-dimensional networks from a related work [39], where we adjusted the last dimension size to scale the network size (ranging from 512 to 4,096 NPUs). The overall list of topologies evaluated in this work is summarized in Table III. Across case studies, as a representative configuration, we chose the 4D-4K topology. Additionally, for corresponding 3D topology evaluations, we utilized the 3D-4K network, which is created by combining two Ring dimensions of the 4D-4K topology.

## VI. RESULT

We conducted several comprehensive design space exploration case studies of multi-dimensional networks to showcase diverse use cases of LIBRA. Due to space constraints, we are highlighting the most interesting design points in each study.

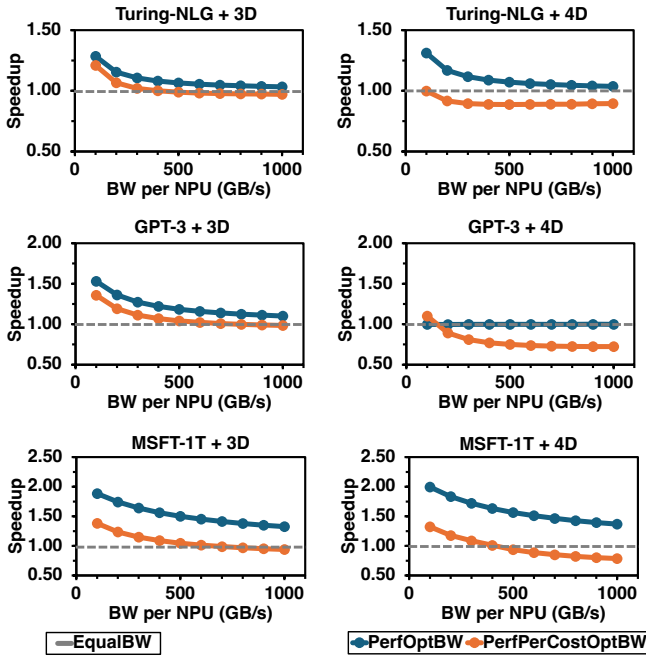


Fig. 13. End-to-end training speedup over the baseline EqualBW. Each point represents a LIBRA-optimized network for the target workload. For example, GPT-3+3D means a 3D network that is optimized for running GPT-3. PerfOptBW network is optimized for maximizing training performance, while PerfPerCostOptBW maximizes perf-per-cost (thereby can have a speedup of less than 1).

#### A. Sweeping Large Model Training

Here, we utilize LIBRA to design a network optimized for a specific training workload.<sup>7</sup> We evaluated both 3D-4K and 4D-4K networks. Additionally, we swept over the BW per NPU in the range of 100–1,000 GB/s, as it can cover the BW budget of recent ML clusters [33], [37], [38].

**Performance.** The performance benefit represented by the speedup over the baseline EqualBW configuration, for training Turing-NLG, GPT-3 and MSFT-1T models over PerfOptBW and PerfPerCostOptBW-optimized networks, is depicted in Fig. 13. Comparing the BW optimization schemes, we observe that *PerfOptBW consistently provides the best performance*. On average, PerfOptBW achieves a  $1.23\times$  speedup ( $2.00\times$  max) compared to the EqualBW network. Note that for GPT-3 on the 4D-4K topology, the training process cannot leverage all Dim 2 BW resources LIBRA assigned, due to the mismatching TP size, thereby yielding performance close to the baseline. Nonetheless, PerfOptBW for this configuration still achieved a  $4.58\times$  perf-per-cost improvement compared to the baseline.

**Perf-per-cost.** The perf-per-cost measurement relative to the baseline EqualBW network, is demonstrated in Fig. 14. PerfPerCostOptBW achieves the highest perf-per-cost for all design points. On average, the perf-per-cost benefit of PerfOptBW and PerfPerCostOptBW over the baseline is  $5.40\times$  ( $12.24\times$  max) and  $9.16\times$  ( $13.02\times$  max), respectively.

**Key Insights.** Larger models exhibit more performance benefits while smaller workloads show higher perf-per-cost ad-

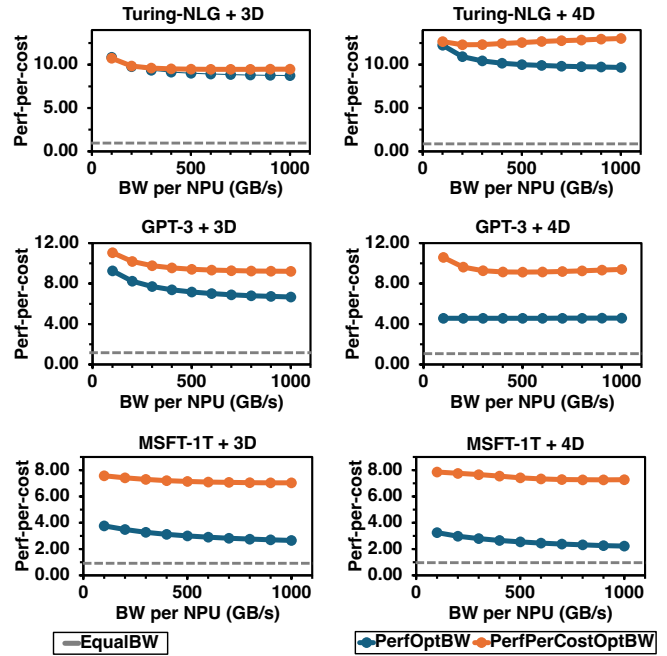


Fig. 14. Perf-per-cost benefit of LIBRA over the EqualBW baseline.

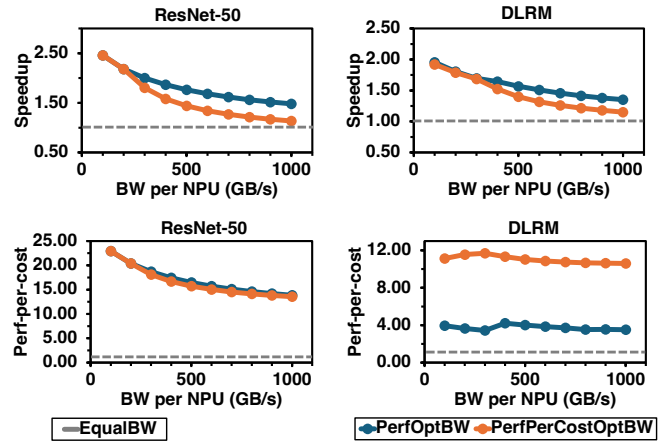


Fig. 15. Speedup and perf-per-cost analysis of ResNet-50 and DLRM model. Results are normalized over corresponding EqualBW baseline.

vantages. Smaller models are less communication-critical, therefore, optimizing the network has a limited impact on performance. As workload sizes tend to increase, judicious design time considerations of LIBRA would gain more importance.

**Non-Transformer Workloads.** LIBRA can optimize the network for non-transformer workloads without any modification. For ResNet-50 and DLRM, we optimized the 4D-4K network using both PerfOptBW and PerfPerCostOptBW objectives. The results are summarized in Fig. 15. It is worth noting that the ResNet-50 model, due to its relatively small size compared to large LLMs, yields very small numbers as its estimated training time. This makes the perf-per-cost metric heavily cost-dependent. Due to the intrinsic numerical instability of the QP solver, PerfPerCostOptBW generated network designs with similar perf-per-cost to PerfOptBW. Nonetheless, PerfPerCostOptBW takes the network cost into consideration during the optimization process, resulting in network designs

<sup>7</sup>In practice, LIBRA is envisioned to design networks optimized for an ensemble of training models. This scenario is shown in Sec. VI-B.



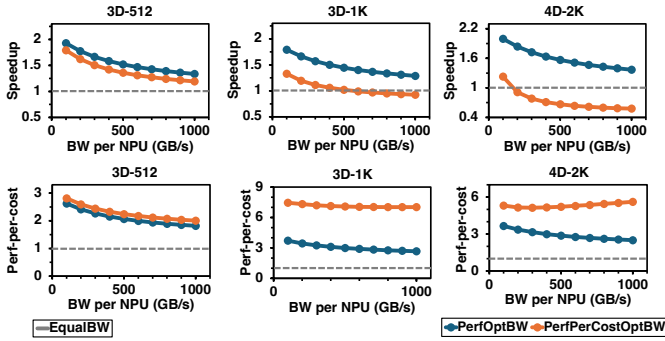


Fig. 16. Speedup and perf-per-cost analysis of MSFT-1T over 3D-512, 3D-1K, and 4D-2K topologies. Results are normalized over their corresponding EqualBW baseline.

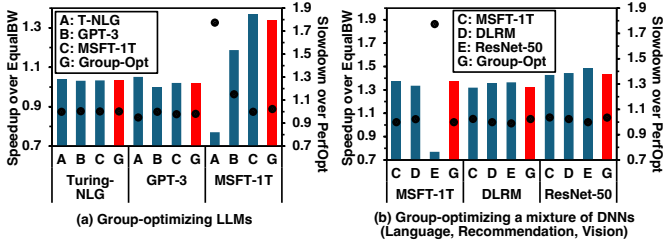


Fig. 17. Speedup (over EqualBW, in bars) and slowdown (over LIBRA-optimized network, in dots) of various DNN models. The red bars denote performance over the group-optimized network. (a) group-optimization among LLMs (b) group-optimization across a mixture of DNNs.

that are 15.41% cheaper on average compared to PerfOptBW.

**Topology Exploration.** LIBRA supports networks of various shapes and scales. In order to showcase how LIBRA operates for a variety of target networks, we also compared three distinct networks with different dimensionality, size, and shape implications: 3D-512, 3D-1K, and 4D-2K. We ran LIBRA using the MSFT-1T workload and compared the speedup and perf-per-cost benefit over their corresponding EqualBW baseline. The results are summarized in Fig. 16.

### B. Optimizing for Multiple Workloads

LIBRA can assist in designing a network by considering a group of workloads, rather than just a single target. For the 4D-4K network with 1,000 GB/s per NPU, we ran PerfOptBW to design networks optimized for specific targets. Then, we ran other non-targeted workloads on these networks to observe slowdowns compared to the training time over the optimized network. Additionally, we evaluated the network designed by LIBRA by considering all target networks at once during the optimization (i.e., group-optimization). We summarize the speedup (over baseline EqualBW) and slowdown (over LIBRA-optimized networks) in Fig. 17. When we optimized the network separately for ResNet-50, DLRM, Turing-NLG, GPT-3, and MSFT-1T, and performed non-optimized model training over them, we observed slowdowns of up to  $1.77\times$ ,  $1.02\times$ ,  $1.77\times$ ,  $1.15\times$ , and  $1.04\times$ , respectively. However, when leveraging all target models jointly to optimize the network, this network achieved near-optimal performance across all workloads, achieving the average slowdown of only  $1.01\times$ .

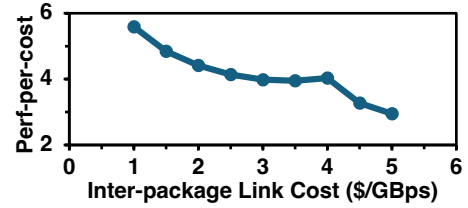


Fig. 18. Normalized perf-per-cost (over baseline EqualBW) benefit of PerfPerCostOptBW on the 4D-4K network, while sweeping the inter-Package link cost from \$1/GBps to \$5/GBps.

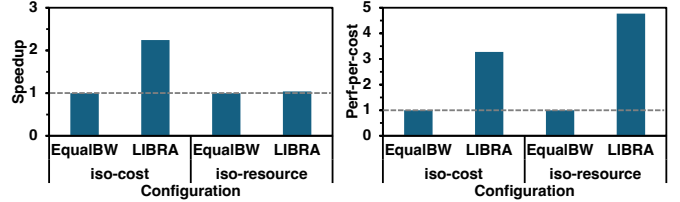


Fig. 19. Normalized performance and perf-per-cost of LIBRA-optimized 4D-4K network (over EqualBW), when Themis runtime optimizer is leveraged for both networks.

### C. Cost Model Sensitivity Analysis

LIBRA’s cost model is a user-defined input, offering maximum flexibility since the cost model can change as technology evolves. To showcase this flexibility, we conduct a sensitivity analysis by varying the inter-Package link costs. We evaluated 4D-4K network with a BW budget of 1,000 GB/s per NPU. We used PerfPerCostOptBW while changing the inter-Package link cost from \$1–\$5/GBps. The resulting perf-per-cost (over baseline EqualBW) is depicted in Fig. 18. On average, the benefit over the EqualBW is  $4.06\times$  ( $5.59\times$  max).

### D. LIBRA with Runtime Optimizations

Since the benefits of runtime-based optimizations are fundamentally determined by their underlying system configurations, incorporating careful design time considerations using LIBRA can enhance their efficacy.

**LIBRA+Themis.** Themis [39] is a recently proposed collective scheduler that optimizes network BW utilization. It dynamically schedules data chunks over multi-dimensional networks in a greedy-based manner. To measure the joint benefit, we trained GPT-3 with Themis using 4D-4K topology, one configured with EqualBW and the other using LIBRA. We evaluated two distinct setups:

- iso-cost: both topologies have the cost of \$15M
- iso-resource: both topologies have 1,000 GB/s per NPU

The normalized performance and perf-per-cost are shown in Fig. 19. For iso-cost, the LIBRA-designed network was able to support  $5.05\times$  more BW per NPU compared to the EqualBW network. Consequently, even with Themis enabled for both systems, the LIBRA-designed network yielded a  $2.24\times$  training speedup. For iso-resource, the LIBRA-designed network showed a  $1.04\times$  better performance over the EqualBW-configured topology, while achieving  $4.58\times$  network cost reduction, leading to a  $4.77\times$  better perf-per-cost.

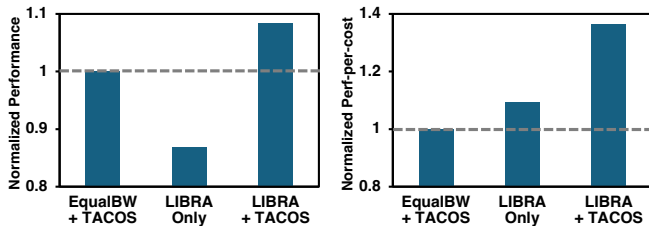


Fig. 20. Normalized performance and perf-per-cost when jointly leveraging TACOS runtime collective synthesizer. LIBRA-only and LIBRA+TACOS results are normalized over EqualBW+TACOS.

**LIBRA+TACOS.** TACOS [63] is a runtime-based tool that can automatically synthesize topology-aware collective algorithms. To demonstrate the co-design opportunities, a 1GB All-Reduce with 8 chunks was synthesized and run over the 3D-Torus network at 1,000 GB/s per NPU. The normalized performance and perf-per-cost are shown in Fig. 20. LIBRA+TACOS showed  $1.25\times$  and  $1.08\times$  speedup over the LIBRA-only and TACOS-only, respectively. Notably, due to the dollar-cost benefit from LIBRA, LIBRA+TACOS exhibited a  $1.36\times$  better perf-per-cost over the TACOS-only setup.

#### E. Co-optimizing Network and Parallelization

LIBRA offers the opportunity for joint co-optimization of the network and target workloads. In this study, we explore the impact of co-optimizing both the parallelization strategy and the network. To investigate this, we modify the TP-DP sizes, resulting in various parallelization strategies for the 4D-4K network with 1,000 GB/s per NPU. For this experiment, we relax the constraint of limited NPU memory and instead assume that the NPUs have access to an extended memory capacity through technologies such as CXL [64] or CPU memory [65]. In Fig. 21, we present the performance of LIBRA’s PerfOptBW network normalized over the baseline using the EqualBW network with HP-(128, 32) parallelization, while varying the parallelization strategies between HP-(8, 512) and HP-(256, 16) for the MSFT-1T workload. As depicted in the figure, we achieve peak training performance with the 4D-4K network using HP-(64, 64). For the co-optimized 4D-4K network, MSFT-1T training was  $1.19\times$  faster compared to the baseline configuration.

**Key Insights.** Training performance significantly degrades when the TP size decreases below 32. This outcome arises from the intricate interplay between TP and DP communication for different parallelization strategies. The total network communication size is minimized when using HP-(32, 128). However, for HP-(64, 64), LIBRA was still able to configure a network that significantly reduced DP time while mitigating the increase in TP time. For other parallelizations, the total communication size was significantly higher due to increased TP or DP communications, resulting in reduced training performance even with LIBRA support.

## VII. RELATED WORK

**Multi-dimensional Networks.** Multi-dimensional networks have been utilized in general-purpose HPC platforms, including 3–6D networks [66]–[68]. However, these networks were

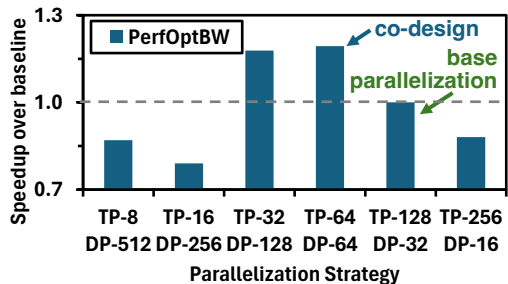


Fig. 21. Normalized speedup of MSFT-1T across various parallelization strategies. All results are normalized to EqualBW with HP-(128, 32). HP-(64, 64) parallelization, along with its co-optimized PerfOptBW network, demonstrates the best training performance.

not specifically designed for AI training. In the AI domain, 3D [9], [37], [38] and 4D [4] networks are being explored.

**Design-Time Optimization.** Collectives differ from point-to-point messages as all NPUs communicate synchronously, and message sizes change throughout the process. Such communication behavior becomes even more complex when using multi-dimensional algorithms. Various topology-aware collective algorithms have been proposed [69]–[74]; however, they are not specifically AI-aware and do not consider workloads, parallelizations, training loops, or network constraints. To the best of our knowledge, this is the first work targeting multi-dimensional network BW optimization for AI workloads at design-time. Another set of proposals offloads collectives to network switches [20], [56] or NICs [23], which are orthogonal to LIBRA. We have incorporated these offload features in our modeling to find the best network BW.

**Co-optimization.** AI HPC clusters are being co-optimized alongside their target workloads due to the substantial resource demand. EFLOPS [75] proposes both a novel network topology and collective algorithm to optimize All-Reduce collectives. ZionEx [13] is a training cluster specifically aimed at accelerating DLRM training tasks. We also demonstrate that runtime-based optimizations perform at their best when leveraged with careful design-time considerations using LIBRA.

## VIII. CONCLUSION

In this paper, we propose LIBRA, a design-time framework to construct workload-aware multi-dimensional networks. To the best of our knowledge, this is the first framework in the field of ML to optimize the BW of a multi-dimensional network, at design-time, using target workload characteristics. LIBRA aims to maximize the training performance and perf-per-cost of a target set of DNN workloads.

## ACKNOWLEDGMENT

This work was supported through awards from Intel. Additionally, this work has been developed and maintained with the support from Semiconductor Research Corporation (SRC), the SRC AIHW program, as well as ACE Center for Evolvable Computing, one of the seven centers of the SRC JUMP 2.0 program. We also extend our sincere appreciation to the reviewers for dedicating their time and providing insightful comments that contributed to the improvement of this paper.

## REFERENCES

- [1] OpenAI, “Introducing chatgpt,” <https://openai.com/blog/chatgpt>, 2022.
- [2] Google DeepMind, “Welcome to the gemini era,” <https://deepmind.google/technologies/gemini>, 2023.
- [3] Microsoft, “Microsoft Copilot: Your everyday ai companion,” <https://copilot.microsoft.com>, 2023.
- [4] Google, “Cloud tpu,” <https://cloud.google.com/tpu>, 2021.
- [5] Intel, “Habana,” <https://habana.ai>, 2021.
- [6] K. Lee and S. Sengupta, “Introducing the ai research supercluster – meta’s cutting-edge ai supercomputer for ai research,” <https://ai.facebook.com/blog/ai-rsc>, 2022.
- [7] T. P. Morgan, “Inside tesla’s innovative and homegrown “dojo” ai supercomputer,” <https://www.nextplatform.com/2022/08/23/inside-tesla-innovative-and-homegrown-dojo-ai-supercomputer>, 2022.
- [8] Cerebras Systems, “Cerebras Systems: Achieving industry best ai performance through a systems approach,” <https://cerebras.net/wp-content/uploads/2021/04/Cerebras-CS-2-Whitepaper.pdf>, 2021.
- [9] D. Patel, “Tensorflow wormhole analysis - a scale out architecture for machine learning that could put nvidia on their back foot,” <https://www.semianalysis.com/p/tensorflow-wormhole-analysis-a-scale>, 2021.
- [10] N. P. Jouppi, C. Young, N. Patil, D. Patterson, G. Agrawal, R. Bajwa, S. Bates, S. Bhatia, N. Boden, A. Borchers, R. Boyle, P.-I. Cantin, C. Chao, C. Clark, J. Coriell, M. Daley, M. Dau, J. Dean, B. Gelb, T. V. Ghaemmaghami, R. Gottipati, W. Gulland, R. Hagmann, C. R. Ho, D. Hogberg, J. Hu, R. Hundt, D. Hurt, J. Ibarz, A. Jaffey, A. Jaworski, A. Kaplan, H. Khaitan, D. Killebrew, A. Koch, N. Kumar, S. Lacy, J. Laudon, J. Law, D. Le, C. Leary, Z. Liu, K. Lucke, A. Lundin, G. MacKean, A. Maggiore, M. Mahony, K. Miller, R. Nagarajan, R. Narayanaswami, R. Ni, K. Nix, T. Norrie, M. Omernick, N. Penukonda, A. Phelps, J. Ross, M. Ross, A. Salek, E. Samadiani, C. Severn, G. Sizikov, M. Snellman, J. Souter, D. Steinberg, A. Swing, M. Tan, G. Thorson, B. Tian, H. Toma, E. Tuttle, V. Vasudevan, R. Walter, W. Wang, E. Wilcox, and D. H. Yoon, “In-datacenter performance analysis of a tensor processing unit,” in *Proceedings of the 44th Annual International Symposium on Computer Architecture (ISCA ’17)*, 2017, p. 1–12.
- [11] Intel, “Gaudi training platform white paper,” <https://habana.ai/wp-content/uploads/2019/06/Habana-Gaudi-Training-Platform-whitepaper.pdf>, 2019.
- [12] Videocardz, “Tesla d1 chip features 50 billion transistors, scales up to 1.1 exaflops with exapod,” <https://videocardz.com/newz/tesla-d1-chip-features-50-billion-transistors-scales-up-to-1-1-exaflops-with-exapod>, 2021.
- [13] D. Mudigere, Y. Hao, J. Huang, Z. Jia, A. Tulloch, S. Sridharan, X. Liu, M. Ozdal, J. Nie, J. Park, L. Luo, J. A. Yang, L. Gao, D. Ivchenko, A. Basant, Y. Hu, J. Yang, E. K. Ardestani, X. Wang, R. Komuravelli, C.-H. Chu, S. Yilmaz, H. Li, J. Qian, Z. Feng, Y. Ma, J. Yang, E. Wen, H. Li, L. Yang, C. Sun, W. Zhao, D. Melts, K. Dhulipala, K. Kishore, T. Graf, A. Eisenman, K. K. Matam, A. Gangidi, G. J. Chen, M. Krishnan, A. Nayak, K. Nair, B. Muthiah, M. khorashadi, P. Bhattacharya, P. Lapukhov, M. Naumov, A. Mathews, L. Qiao, M. Smelyanskiy, B. Jia, and V. Rao, “Software-hardware co-design for fast and scalable training of deep learning recommendation models,” in *Proceedings of the 49th Annual International Symposium on Computer Architecture (ISCA ’22)*, 2022, p. 993–1011.
- [14] M. Naumov, D. Mudigere, H.-J. M. Shi, J. Huang, N. Sundaraman, J. Park, X. Wang, U. Gupta, C.-J. Wu, A. G. Azzolini, D. Dzhulgakov, A. Mallevich, I. Cherniavskii, Y. Lu, R. Krishnamoorthi, A. Yu, V. Kondratenko, S. Pereira, X. Chen, W. Chen, V. Rao, B. Jia, L. Xiong, and M. Smelyanskiy, “Deep learning recommendation model for personalization and recommendation systems,” in *arXiv:1906.00091 [cs.IR]*, 2019.
- [15] V. Sze, Y.-H. Chen, J. Emer, A. Suleiman, and Z. Zhang, “Hardware for machine learning: Challenges and opportunities,” in *Proceedings of the 2017 IEEE Custom Integrated Circuits Conference (CICC’ 17)*. Ieee, 2017, pp. 1–8.
- [16] T. Krishna, H. Kwon, A. Parashar, M. Pellauer, and A. Samajdar, “Data orchestration in deep learning accelerators,” 2020.
- [17] T. Brown, B. Mann, N. Ryder, M. Subbiah, J. D. Kaplan, P. Dhariwal, A. Neelakantan, P. Shyam, G. Sastry, A. Askell, S. Agarwal, A. Herbert-Voss, G. Krueger, T. Henighan, R. Child, A. Ramesh, D. Ziegler, J. Wu, C. Winter, C. Hesse, M. Chen, E. Sigler, M. Litwin, S. Gray, B. Chess, J. Clark, C. Berner, S. McCandlish, A. Radford, I. Sutskever, and D. Amodei, “Language models are few-shot learners,” in *Proceedings of the Advances in Neural Information Processing Systems 33 (NeurIPS ’20)*, vol. 33, 2020, pp. 1877–1901.
- [18] Meta, “Fully Sharded Data Parallel: faster ai training with fewer gpus,” <https://engineering.fb.com/2021/07/15/open-source/fsdp>, 2021.
- [19] B. Klenk, N. Jiang, G. Thorson, and L. Dennison, “An in-network architecture for accelerating shared-memory multiprocessor collectives,” in *Proceedings of the 47th Annual International Symposium on Computer Architecture (ISCA ’20)*, 2020, pp. 996–1009.
- [20] Y. Li, I.-J. Liu, Y. Yuan, D. Chen, A. Schwing, and J. Huang, “Accelerating distributed reinforcement learning with in-switch computing,” in *Proceedings of the 46th International Symposium on Computer Architecture (ISCA ’19)*, 2019, p. 279–291.
- [21] A. Sapio, M. Canini, C. Ho, J. Nelson, P. Kalnis, C. Kim, A. Krishnamurthy, M. Moshref, D. R. K. Ports, and P. Richtárik, “Scaling distributed machine learning with in-network aggregation,” in *arXiv:1903.06701 [cs.DC]*, 2019.
- [22] Y. Mikami, H. Suganuma, P. Uchupala, Y. Tanaka, and Y. Kageyama, “Massively Distributed SGD: Imagenet/resnet-50 training in a flash,” in *arXiv:1811.05233 [cs.LG]*, 2019.
- [23] S. Rashidi, M. Denton, S. Sridharan, S. Srinivasan, A. Suresh, J. Nie, and T. Krishna, “Enabling compute-communication overlap in distributed deep learning training platforms,” in *Proceedings of the 48th Annual International Symposium on Computer Architecture (ISCA ’21)*, 2021, pp. 540–553.
- [24] I. Cutress, “Analyzing Intel’s Discrete Xe-HPC Graphics Disclosure: Ponte vecchio, rambo cache, and gelato,” <https://www.anandtech.com/show/15188/analyzing-intels-discrete-xe-hpc-graphics-disclosure-ponte-vecchio/5>, 2019.
- [25] NVIDIA, “Nvlink and nvswhitch,” <https://www.nvidia.com/en-us/data-center/nvlink>, 2022.
- [26] —, “Connectx nics,” <https://www.nvidia.com/en-in/networking/ethernet-adapters>, 2021.
- [27] —, “The nvidia quantum infiniband platform,” <https://www.nvidia.com/en-us/networking/products/infiniband>, 2023.
- [28] J. Kaplan, S. McCandlish, T. Henighan, T. B. Brown, B. Chess, R. Child, S. Gray, A. Radford, J. Wu, and D. Amodei, “Scaling laws for neural language models,” in *arXiv:2001.08361 [cs.LG]*, 2020.
- [29] Cisco, “Co-packaged optics and an open ecosystem,” <https://blogs.cisco.com/sp/co-packaged-optics-and-an-open-ecosystem>, 2021.
- [30] A. Arunkumar, E. Bolotin, B. Cho, U. Milic, E. Ebrahimi, O. Villa, A. Jaleel, C.-J. Wu, and D. Nellans, “MCM-GPU: Multi-chip-module gpus for continued performance scalability,” in *Proceedings of the 44th Annual International Symposium on Computer Architecture (ISCA’ 17)*, 2017, pp. 320–332.
- [31] Y. S. Shao, J. Clemons, R. Venkatesan, B. Zimmer, M. Fojtik, N. Jiang, B. Keller, A. Klinefelter, N. Pinckney, P. Raina, S. G. Tell, Y. Zhang, W. J. Dally, J. Emer, C. T. Gray, B. Khailany, and S. W. Keckler, “Simba: Scaling deep-learning inference with multi-chip-module-based architecture,” in *Proceedings of the 52nd Annual IEEE/ACM International Symposium on Microarchitecture (MICRO ’52)*, 2019, p. 14–27.
- [32] S. Pal, D. Petrisco, M. Tomei, P. Gupta, S. S. Iyer, and R. Kumar, “Architecting waferscale processors - a gpu case study,” in *Proceedings of the 2019 IEEE International Symposium on High Performance Computer Architecture (HPCA ’19)*, 2019, pp. 250–263.
- [33] N. Jouppi, G. Kurian, S. Li, P. Ma, R. Nagarajan, L. Nai, N. Patil, S. Subramanian, A. Swing, B. Towles, C. Young, X. Zhou, Z. Zhou, and D. A. Patterson, “TPU v4: An optically reconfigurable supercomputer for machine learning with hardware support for embeddings,” in *Proceedings of the 50th Annual International Symposium on Computer Architecture (ISCA ’23)*, 2023.
- [34] Lightmatter, “Passage: A wafer-scale, programmable photonic interconnect,” <https://lightmatter.co/products/passage>, 2023.
- [35] Intel, “Intel data center gpu max series technical overview,” <https://www.intel.com/content/www/us/en/developer/articles/technical/intel-data-center-gpu-max-series-overview.html>, 2023.
- [36] NVIDIA, “NVIDIA DGX-2: The world’s most powerful deep learning system for the most complex ai challenges,” <https://www.nvidia.com/content/dam/en-zz/Solutions/Data-Center/dgx-1/dgx-2-datasheet-us-nvidia-955420-r2-web-new.pdf>, 2019.
- [37] —, “Nvidia a100 tensor core gpu,” <https://www.nvidia.com/en-us/data-center/a100>, 2021.
- [38] —, “Nvidia h100 tensor core gpu,” <https://www.nvidia.com/en-us/data-center/h100>, 2022.

- [39] S. Rashidi, W. Won, S. Srinivasan, S. Sridharan, and T. Krishna, "Themis: A network bandwidth-aware collective scheduling policy for distributed training of dl models," in *Proceedings of the 49th Annual International Symposium on Computer Architecture (ISCA '22)*, 2022, p. 581–596.
- [40] S. Coll, E. Frachtenberg, F. Petrini, A. Hoisie, and L. Gurvits, "Using multirail networks in high-performance clusters," in *Proceedings of the 2001 IEEE International Conference on Cluster Computing (CLUSTER '01)*, 2001, pp. 15–24.
- [41] N. Wolfe, M. Mubarak, N. Jain, J. Domke, A. Bhatele, C. D. Carothers, and R. B. Ross, "Preliminary performance analysis of multi-rail fat-tree networks," in *Proceedings of the 17th IEEE/ACM International Symposium on Cluster, Cloud and Grid Computing (CCGRID '17)*, 2017, pp. 258–261.
- [42] R. Smith, "Spotted At Hot Chips: Quad tile intel xe-hp gpu," <https://www.anandtech.com/show/15996/spotted-at-hot-chips-quad-tile-intel-xehp-gpu>, 2020.
- [43] S. Rajbhandari, J. Rasley, O. Ruwase, and Y. He, "ZeRO: Memory optimizations toward training trillion parameter models," in *arXiv:1910.02054 [cs.LG]*, 2020.
- [44] J. Verbraeken, M. Wolting, J. Katzy, J. Kloppenburg, T. Verbelen, and J. S. Rellermeyer, "A survey on distributed machine learning," *ACM Comput. Surv.*, vol. 53, no. 2, 2020.
- [45] M. Shoeybi, M. Patwary, R. Puri, P. LeGresley, J. Casper, and B. Catanzaro, "Megatron-LM: Training multi-billion parameter language models using model parallelism," in *arXiv:1909.08053 [cs.CL]*, 2019.
- [46] S. Rashidi, S. Sridharan, S. Srinivasan, and T. Krishna, "ASTRA-SIM: Enabling sw/hw co-design exploration for distributed dl training platforms," in *Proceedings of the 2020 IEEE International Symposium on Performance Analysis of Systems and Software (ISPASS '20)*, 2020, pp. 81–92.
- [47] NVIDIA, "Nvidia collective communication library (nccl)," <https://developer.nvidia.com/nccl>, 2017.
- [48] Intel, "Intel oneapi collective communications library," <https://www.intel.com/content/www/us/en/developer/tools/oneapi/oneccl.html>, 2020.
- [49] R. Thakur, R. Rabenseifner, and W. Gropp, "Optimization of collective communication operations in mpich," *Int. J. High Perform. Comput. Appl.*, vol. 19, no. 1, pp. 49–66, 2005.
- [50] M. Cho, U. Finkler, M. Serrano, D. Kung, and H. Hunter, "BlueConnect: Decomposing all-reduce for deep learning on heterogeneous network hierarchy," *IBM J. Res. Dev.*, vol. 63, no. 6, pp. 1–11, 2019.
- [51] S. A. Mojumder, M. S. Louis, Y. Sun, A. K. Ziabari, J. L. Abellan, J. Kim, D. Kaeli, and A. Joshi, "Profiling dnn workloads on a volta-based dgx-1 system," in *Proceedings of the 2018 IEEE International Symposium on Workload Characterization (IISWC '18)*, 2018, pp. 122–133.
- [52] NVIDIA, "NVIDIA DGX SuperPOD: Instant infrastructure for ai leadership," <https://resources.nvidia.com/en-us-auto-datacenter/nvpod-superpod-wp-09>, 2020.
- [53] G. Wang, S. Venkataraman, A. Phanishayee, N. Devanur, J. Thelin, and I. Stoica, "Blink: Fast and generic collectives for distributed ml," in *Proceedings of the 2020 Machine Learning and Systems (MLSys '20)*, vol. 2, 2020, pp. 172–186.
- [54] W. Won, T. Heo, S. Rashidi, S. Sridharan, S. Srinivasan, and T. Krishna, "ASTRA-sim2.0: Modeling hierarchical networks and disaggregated systems for large-model training at scale," in *IEEE International Symposium on Performance Analysis of Systems and Software (ISPASS '23)*, 2023.
- [55] J. Chen, S. Li, R. Gun, J. Yuan, and T. Hoefler, "AutoDDL: Automatic distributed deep learning with asymptotically optimal communication," in *arXiv:2301.06813 [cs.DC]*, 2023.
- [56] R. L. Graham, D. Bureddy, P. Lui, H. Rosenstock, G. Shainer, G. Bloch, D. Goldener, M. Dubman, S. Kotchubievsky, V. Koushnir, L. Levi, A. Margolin, T. Ronen, A. Shpiner, O. Wertheim, and E. Zahavi, "Scalable hierarchical aggregation protocol (SHArP): a hardware architecture for efficient data reduction," in *Proceedings of the First Workshop on Optimization of Communication in HPC (COM-HPC '16)*, 2016, p. 1–10.
- [57] W. Wang, M. Khazraee, Z. Zhong, M. Ghobadi, Z. Jia, D. Mudigere, Y. Zhang, and A. Kewitsch, "TopoOpt: Co-optimizing network topology and parallelization strategy for distributed training jobs," in *Proceedings of the 20th USENIX Symposium on Networked Systems Design and Implementation (NSDI '23)*, 2023, pp. 739–767.
- [58] M. Khani, M. Ghobadi, M. Alizadeh, Z. Zhu, M. S. Glick, K. Bergman, A. Vahdat, B. Klenk, and E. Ebrahimi, "TeraRack: A tbps rack for machine learning training," 2020.
- [59] Gurobi Optimization, "Gurobi optimizer," <https://www.gurobi.com/solutions/gurobi-optimizer>, 2023.
- [60] ASTRA-sim, "Astra-sim validation," <https://astra-sim.github.io/astra-sim-docs/validation/validation.html>, 2023.
- [61] A. Vaswani, N. Shazeer, N. Parmar, J. Uszkoreit, L. Jones, A. N. Gomez, L. u. Kaiser, and I. Polosukhin, "Attention is all you need," in *Proceedings of the Advances in Neural Information Processing Systems 30 (NIPS '17)*, vol. 30, 2017.
- [62] K. He, X. Zhang, S. Ren, and J. Sun, "Deep residual learning for image recognition," in *Proceedings of the 2016 IEEE Conference on Computer Vision and Pattern Recognition (CVPR '16)*, 2016, pp. 770–778.
- [63] W. Won, M. Elavazhagan, S. Srinivasan, A. Durg, S. Gupta, and T. Krishna, "TACOS: Topology-aware collective algorithm synthesizer for distributed training," in *arXiv:2304.05301 [cs.DC]*, 2023.
- [64] M. Wagh, "Introducing Compute Express Link (CXL) 3.0: Expanding fabric capabilities and management," [https://www.openfabrics.org/wp-content/uploads/2023-workshop/2023-workshop-presentations/day-2/2023\\_MWagh.pdf](https://www.openfabrics.org/wp-content/uploads/2023-workshop/2023-workshop-presentations/day-2/2023_MWagh.pdf), 2023.
- [65] S. Rajbhandari, C. Li, Z. Yao, M. Zhang, R. Y. Aminabadi, A. A. Awan, J. Rasley, and Y. He, "DeepSpeed-MoE: Advancing mixture-of-experts inference and training to power next-generation ai scale," in *arXiv:2201.05596 [cs.LG]*, 2022.
- [66] R. Alverson, D. Roweth, and L. Kaplan, "The gemini system interconnect," in *Proceedings of the 18th IEEE Symposium on High Performance Interconnects (HOTI '10)*, 2010, pp. 83–87.
- [67] D. Chen, N. Easley, P. Heidelberger, S. Kumar, A. Mamidala, F. Petrini, R. Senger, Y. Sugawara, R. Walkup, B. Steinmacher-Burow, A. Choudhury, Y. Sabharwal, S. Singhal, and J. J. Parker, "Looking under the hood of the ibm blue gene/q network," in *Proceedings of the International Conference on High Performance Computing, Networking, Storage and Analysis (SC '12)*, 2012.
- [68] Y. Ajima, S. Sumimoto, and T. Shimizu, "Tofu: A 6d mesh/torus interconnect for exascale computers," *Computer*, vol. 42, no. 11, pp. 36–40, 2009.
- [69] A. J. Peña, R. G. C. Carvalho, J. Dinan, P. Balaji, R. Thakur, and W. Gropp, "Analysis of topology-dependent mpi performance on gemini networks," in *Proceedings of the 20th European MPI Users' Group Meeting (EuroMPI '13)*, 2013, p. 61–66.
- [70] M. J. Rashit, J. Green, P. Balaji, A. Afsahi, and W. Gropp, "Multi-core and network aware mpi topology functions," in *Proceedings of the 18th European MPI Users' Group Meeting (EuroMPI '11)*, 2011, p. 50–60.
- [71] A. Faraj, S. Kumar, B. Smith, A. Mamidala, and J. Gunnels, "MPI Collective Communications on The Blue Gene/P Supercomputer: Algorithms and optimizations," in *Proceedings of the 17th IEEE Symposium on High Performance Interconnects (HOTI '09)*, 2009, pp. 63–72.
- [72] S. Kumar, A. Mamidala, P. Heidelberger, D. Chen, and D. Faraj, "Optimization of mpi collective operations on the ibm blue gene/q supercomputer," *Int. J. High Perform. Comput. Appl.*, vol. 28, no. 4, p. 450–464, 2014.
- [73] G. Almási, P. Heidelberger, C. J. Archer, X. Martorell, C. C. Erway, J. E. Moreira, B. Steinmacher-Burow, and Y. Zheng, "Optimization of mpi collective communication on bluegene/l systems," in *Proceedings of the 19th Annual International Conference on Supercomputing (ICS '05)*, 2005, p. 253–262.
- [74] T. Adachi, N. Shida, K. Miura, S. Sumimoto, A. Uno, M. Kurokawa, F. Shoji, and M. Yokokawa, "The design of ultra scalable mpi collective communication on the k computer," *Computer Science - Research and Development*, vol. 28, 2013.
- [75] J. Dong, Z. Cao, T. Zhang, J. Ye, S. Wang, F. Feng, L. Zhao, X. Liu, L. Song, L. Peng, Y. Guo, X. Jiang, L. Tang, Y. Du, Y. Zhang, P. Pan, and Y. Xie, "EFLOPS: Algorithm and system co-design for a high performance distributed training platform," in *Proceedings of the 2020 IEEE International Symposium on High Performance Computer Architecture (HPCA '20)*, 2020, pp. 610–622.